

Article

Selective Catalytic Oxidation of Toluene to Benzaldehyde: Effect of Aging Time and Calcination Temperature Using $\text{Cu}_x\text{Zn}_y\text{O}$ Mixed Metal Oxide Nanoparticles

Khadijah H. Alharbi ^{1,*}, Ali Alsalmeh ² , Ahmed Bader A. Aloumi ² and Mohammed Rafiq H. Siddiqui ^{2,*} 

¹ Department of Chemistry, Science and Arts College, Rabigh Campus, King Abdulaziz University, Jeddah 21911, Saudi Arabia

² Department of Chemistry, College of Science, King Saud University, P.O. Box 2455, Riyadh 11451, Saudi Arabia; aalsalmeh@ksu.edu.sa (A.A.); aaloumi1@ksu.edu.sa (A.B.A.A.)

* Correspondence: khalharbe@kau.edu.sa (K.H.A.); rafiqs@ksu.edu.sa (M.R.H.S.); Tel.: +966-563180807 (K.H.A.); +966-(0)114676082 (M.R.H.S.)

Abstract: Oxidation is an important organic transformation, and several catalysts have been reported for this conversion. In this study, we report the synthesis of mixed metal oxide $\text{Cu}_x\text{Zn}_y\text{O}$, which is prepared by a coprecipitation method by varying the molar ratio of Cu and Zn in the catalytic system. The prepared mixed metal oxide $\text{Cu}_x\text{Zn}_y\text{O}$ was evaluated for catalytic performance for toluene oxidation. Various parameters of the catalytic evaluation were studied in order to ascertain the optimum condition for the best catalytic performance. The results indicate that aging time, calcination temperature, reaction temperature, and feed rate influence catalytic performance. It was found that the catalyst interfaces apparently enhanced catalytic activity for toluene oxidation. The XRD diffractograms reveal the crystalline nature of the mixed metal oxide formed and also confirm the coexistence of hexagonal and monoclinic crystalline phases. The catalyst prepared by aging for 4 h and calcined at 450 °C was found to be the best for the conversion of toluene to benzaldehyde while the reactor temperature was maintained at 250 °C with toluene fed into the reactor at 0.01 mL/min. The catalyst was active for about 13 h.

Keywords: oxidation of toluene; mixed metal oxide; heterogeneous catalysis



Citation: Alharbi, K.H.; Alsalmeh, A.; Aloumi, A.B.A.; Siddiqui, M.R.H. Selective Catalytic Oxidation of Toluene to Benzaldehyde: Effect of Aging Time and Calcination Temperature Using $\text{Cu}_x\text{Zn}_y\text{O}$ Mixed Metal Oxide Nanoparticles. *Catalysts* **2021**, *11*, 354. <https://doi.org/10.3390/catal11030354>

Academic Editor: Sónia Carabineiro

Received: 26 January 2021

Accepted: 5 March 2021

Published: 9 March 2021

Publisher's Note: MDPI stays neutral with regard to jurisdictional claims in published maps and institutional affiliations.



Copyright: © 2021 by the authors. Licensee MDPI, Basel, Switzerland. This article is an open access article distributed under the terms and conditions of the Creative Commons Attribution (CC BY) license (<https://creativecommons.org/licenses/by/4.0/>).

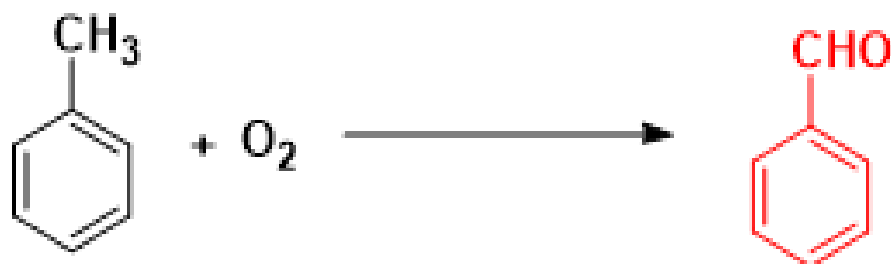
1. Introduction

Toluene, an aromatic hydrocarbon, is a solvent that is an important industrial feedstock. Moreover, it is also an important starting material for the preparation of benzaldehyde and benzyl alcohol. However, this transformation has intrigued scientists for a long time as this oxidation is difficult because of the over oxidation of benzaldehyde into benzoic acid. Hence, the benzoic acid production is carried out by the oxidation of toluene, while the chlorination of toluene is employed for the production of benzaldehyde and benzyl alcohol, which raises serious ecological issues [1–3]. A variety of transition metal catalysts have been reported for the synthesis of benzaldehyde using a variety of substrates as starting materials such as benzyl chloride, benzyl alcohol, and toluene, as mentioned earlier (Scheme 1) [4,5]. However, the preparation of benzaldehyde from toluene oxidation is more efficient for industrial production, and hence it is widely studied.

Various noble-metal-based catalysts such as Au, Pd, Pt, Ru, and Ag, along with their alloys, have been utilized for the oxidation of toluene by oxygen [6–10]. However, in most cases, the selectivity towards benzaldehyde is compromised; moreover, these catalysts are not cost-effective for use in large-scale production. Hence, it can be said that a cheap and efficient catalytic system for high toluene conversion is yet to be identified.

In order to replace the noble metals, cheaper alternatives are being probed by replacing these noble metals with cheaper transition metals for a variety of chemical reactions [11–14].

One such transition metal is Zn, and zinc-based catalysts have been widely used for various conversions such as decomposition of nitrous oxide [15], oxidation of water [16], hydrocarbon oxidation [17], dye degradation [18], and preparation of alcohols [19–22]. On the other hand, copper-based catalysts have also been broadly employed for several conversions, such as CO oxidation [23], benzene oxidation [24], and the hydroxylation of benzene [25].



Scheme 1. Schematic representation of oxidation of toluene.

Mixed metal oxides have also attracted attention for other catalytic reactions such as oxidation, dehydrogenation, and various coupling reactions [26–29]. However, one such mixed metal oxide, zinc–copper mixed oxide catalyst, has gained attention due to its use in a plethora of catalytic processes, particularly for methanol synthesis [30], CO oxidation [31,32], methanol oxidation [33], primary alcohols [34], and reduction of 4-nitrophenol [35]. However, to the best of our knowledge, it has not been employed for the conversion of toluene to benzaldehyde.

Hence, based on the above literature reports and in continuation of our studies towards preparation of various catalysts for different conversion reactions [36–42], in the present work we report the synthesis of $\text{Cu}_x\text{Zn}_y\text{O}$ mixed oxide by coprecipitation with varied aging time and calcination temperature. The prepared catalysts were characterized by various techniques such as XRD, XPS, FT-IR, TGA, SEM, and TEM. The catalysts obtained were studied for the optimization of reaction conditions for the conversion of toluene to benzaldehyde.

2. Results

2.1. XRD Analysis

The $\text{Cu}_x\text{Zn}_y\text{O}$ mixed metal oxide nanoparticles were synthesized by the coprecipitation method and subjected to calcination at different temperatures, namely 350, 450, and 550 °C. The XRD pattern of the samples calcined at different temperatures is presented in Figure 1. No observable difference was found among the three XRD patterns observed.

A comparison of XRD patterns obtained for $\text{Cu}_x\text{Zn}_y\text{O}$ mixed metal oxide nanoparticles calcined at 450 °C with standard peaks is displayed in Figure 2. The high-intensity sharp peak confirmed the highly crystalline nature of the material. The peaks observed completely matched those reported in the database for CuO (JCPDS 48-1548) and ZnO (JCPDS 36-1451). The XRD pattern obtained indicated the absence of any other molecules of Zn and Cu, since there were no additional peaks observed in the XRD pattern. The pattern observed in the ZnO diffractogram at 31.83(100), 34.45(002), 36.30(101), 47.57(012), 56.65(110), 62.90(013), 66.28(200), 68.03(112), 69.11(201), 72.47(004), and 76.97(202) confirmed the formation of hexagonal structure like wurtzite (space group: $P6_3mc$, lattice parameters: $a = 3.2533 \text{ \AA}$ and $c = 5.2073 \text{ \AA}$) [22]. Similarly, the remaining signals at 32.64(110), 35.56(11-1), 38.75(111), 46.26(-112), 48.78(20-2), 53.49(020), 56.63(021), 58.38(202), 61.55(-113), 65.85(022), 66.28(31-1), 68.03(113), 72.45(311), and 75.20(22-2) were confirmed to be of CuO in tenorite crystal with monoclinic crystal structure (space group: $C1c1$, lattice parameters: $a = 4.6893 \text{ \AA}$, $b = 3.4268 \text{ \AA}$, $c = 5.1321 \text{ \AA}$, and $\beta = 99.653^\circ$) [22].

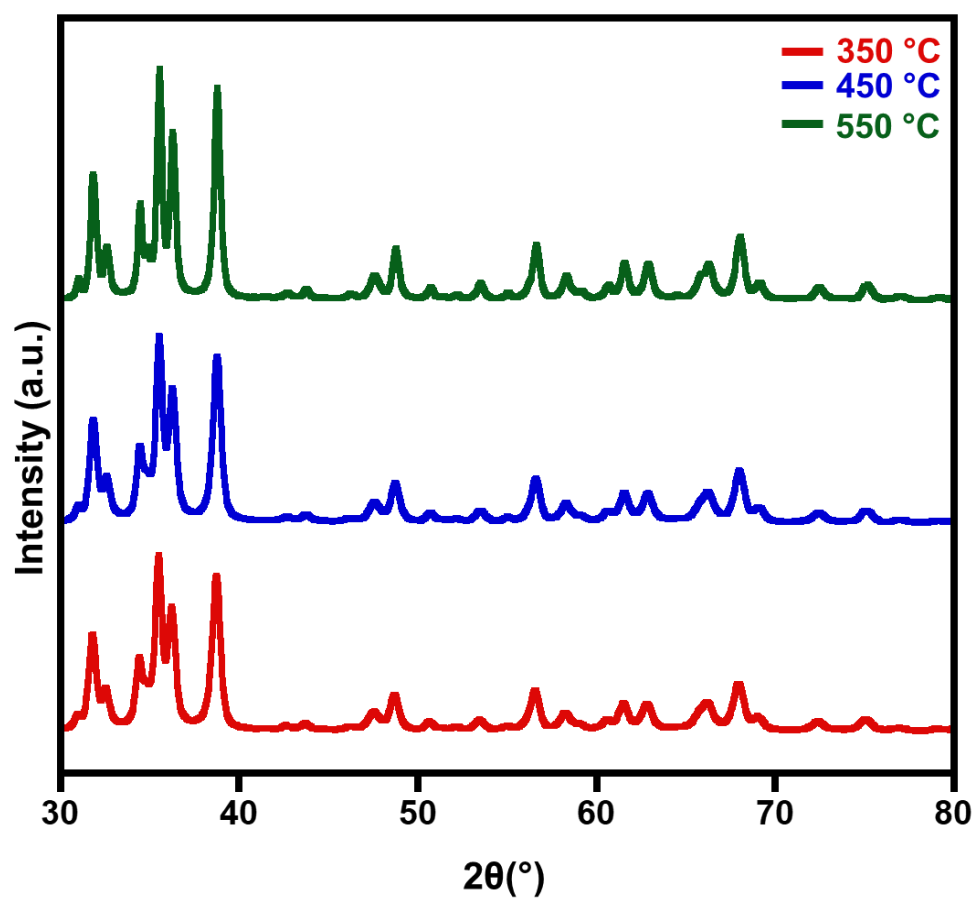


Figure 1. XRD patterns of Cu_xZn_yO mixed metal oxide nanoparticles calcined at 350, 450, and 550 °C.

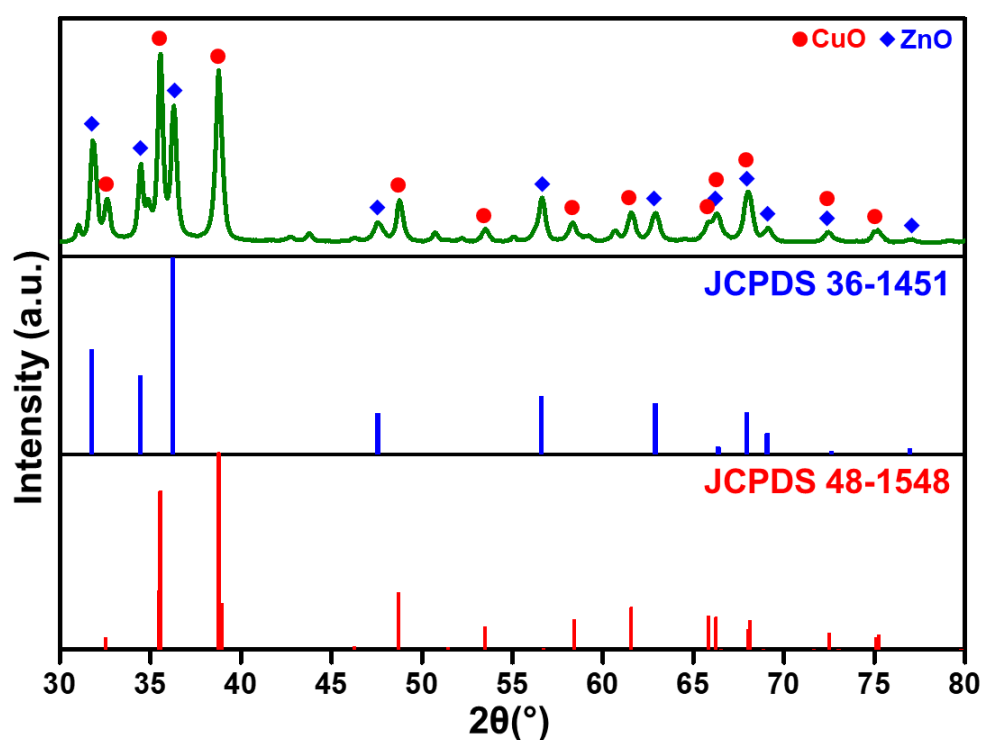


Figure 2. Comparison of XRD pattern of Cu_xZn_yO mixed metal oxide (top) with standard database JCPDS 36-1451 (middle) and JCPDS 48-1548 (bottom).

2.2. TGA Analysis

The thermal stability of the synthesized materials was analyzed using thermogravimetric analysis. Figure 3 represents the TGA analysis pattern of $\text{Cu}_x\text{Zn}_y\text{O}$ mixed metal oxide nanoparticles after being calcined at 350, 450, and 550 °C. All the samples were heated from room temperature to 800 °C and found to be highly stable under N_2 flow atmosphere. $\text{Cu}_x\text{Zn}_y\text{O}$ mixed metal oxide nanoparticles calcined at 350 and 450 °C exhibited an almost similar pattern. A weight loss of ~3% was observed for both of the materials, with a continuous small weight reduction from beginning to end. However, a comparatively larger detriment was seen until 200 °C. This loss in weight might be attributed to the removal of absorbed moieties such as moisture and volatile impurities [19]. Another decay dip was observed in the temperature range between 550 and 700 °C. The decay was only ~0.4%, which might be due to the degradation of the hydroxides or carbonates of zinc and copper [11]. $\text{Cu}_x\text{Zn}_y\text{O}$ mixed metal oxide nanoparticles calcined at 550 °C displayed a TGA pattern below 200 °C similar to those of nanoparticles calcined at 350 and 450 °C. Above 200 °C, a weight loss of only ~0.5% was observed in $\text{Cu}_x\text{Zn}_y\text{O}$ mixed metal oxide nanoparticles calcined at 550 °C until the temperature of TGA analysis reached 800 °C.

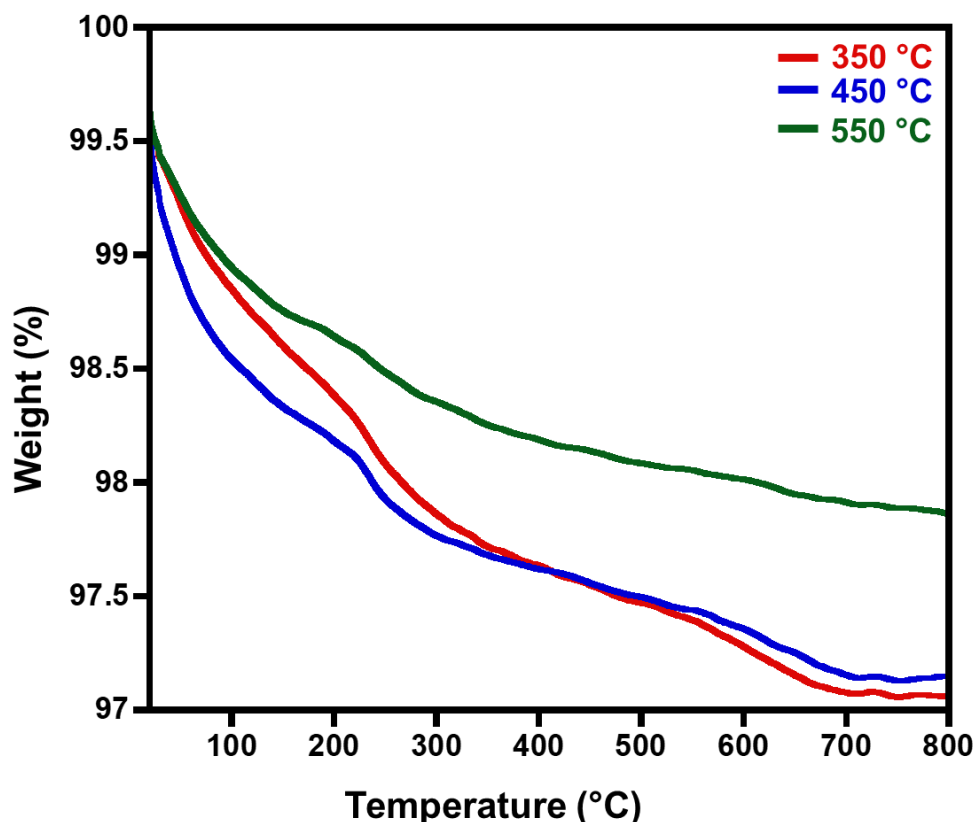


Figure 3. TGA analysis of $\text{Cu}_x\text{Zn}_y\text{O}$ mixed metal oxide nanoparticles calcined at 350, 450, and 550 °C.

2.3. SEM Analysis

The surface morphology of $\text{Cu}_x\text{Zn}_y\text{O}$ mixed metal oxide nanoparticles calcined at 350, 450, and 550 °C was investigated using an SEM analytical technique. Figure 4 exhibits the SEM images of $\text{Cu}_x\text{Zn}_y\text{O}$ mixed metal oxide nanoparticles calcined at 350, 450, and 550 °C. An agglomeration of nanoparticles was observed in the materials calcined at three different temperatures. There was no significant structural difference found in the surface morphology among the materials calcined at three different temperatures. It can be concluded from the images of three different calcined $\text{Cu}_x\text{Zn}_y\text{O}$ materials that the calcination of the material at 350, 450, and 550 °C did not alter the surface morphology. An EDX analysis technique attached to SEM was used to estimate the composition of

the materials synthesized. The elemental composition of $\text{Cu}_x\text{Zn}_y\text{O}$ mixed metal oxide nanoparticles calcined at 350, 450, and 550 °C is displayed in Table 1. The percentages of elements and CuO and ZnO in the mixed metal oxide revealed the composition expected given the concentrations of the starting materials used in the preparation.

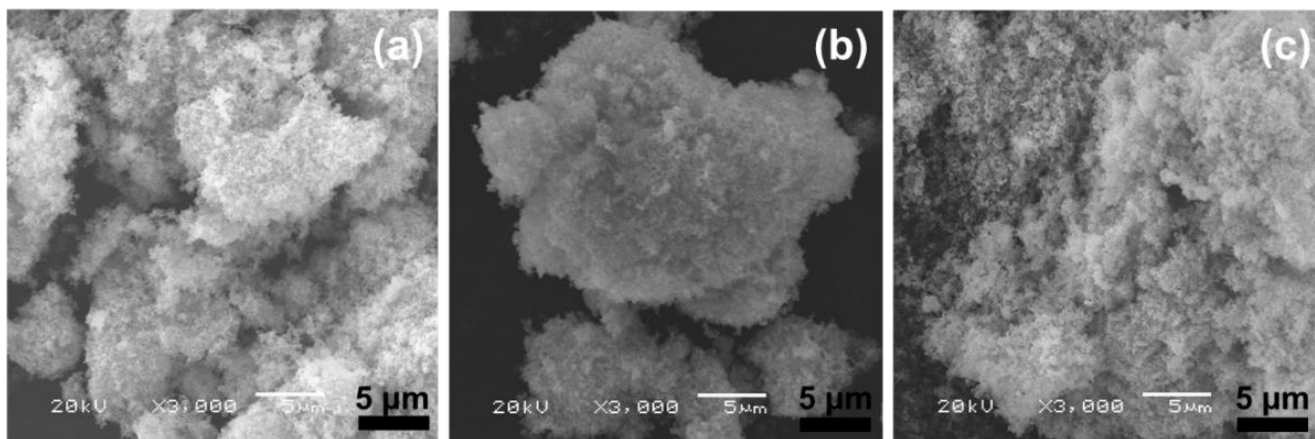


Figure 4. SEM images of $\text{Cu}_x\text{Zn}_y\text{O}$ mixed metal oxide nanoparticles calcined at (a) 350 °C, (b) 450 °C, and (c) 550 °C.

Table 1. EDX analysis data obtained for $\text{Cu}_x\text{Zn}_y\text{O}$ mixed metal oxide nanoparticles calcined at 350, 450, and 550 °C.

Calcination Temperature (°C)	Mass (%)				
	Elemental			Compound	
	Cu	Zn	O	CuO	ZnO
350	49.08	30.98	19.94	61.43	38.57
450	51.50	28.54	19.95	64.47	35.53
550	50.28	29.78	19.95	62.93	37.07

2.4. TEM Analysis

To further investigate particle shape and size, TEM was utilized. Figure 5a–c represents the TEM images of $\text{Cu}_x\text{Zn}_y\text{O}$ mixed metal oxide nanoparticles calcined at 350, 450, and 550 °C. A mixture of spherical and cylindrical nanoparticles was observed in the nanoparticles formed. The particle size of the prepared nanomaterials was elucidated from the TEM images in Figure 5a–c using ImageJ software. A particle size distribution graph of $\text{Cu}_x\text{Zn}_y\text{O}$ mixed metal oxide nanoparticles calcined at 350, 450, and 550 °C is represented in Figure 5d–f. From the image, it can be concluded that as the calcination temperature increased, the size of the nanoparticle also increased, and it was found to be 22.7, 28.1, and 37.2 nm for nanoparticles calcined at 350, 450, and 550 °C, respectively.

2.5. XPS Analysis

XPS analysis of the $\text{Cu}_x\text{Zn}_y\text{O}$ catalyst prepared was carried out to further ascertain the composition of the as-prepared catalyst and to understand the oxidation state of the Cu and Zn in the mixed metal oxide. Figure 6 gives the survey scan of the catalyst confirming the elemental composition of the as-prepared catalyst. The XPS spectra of the Zn 2p and Cu 2p revealed that the binding energies of 1026 and 1048 eV correspond to Zn 2p_{3/2} and Zn 2p_{1/2}, respectively, and 938 and 945 eV correspond to Cu 2p_{3/2} and Cu 2p_{1/2} core levels, respectively [43–45]. The binding energies indicate that both copper and zinc are in +2 oxidation state.

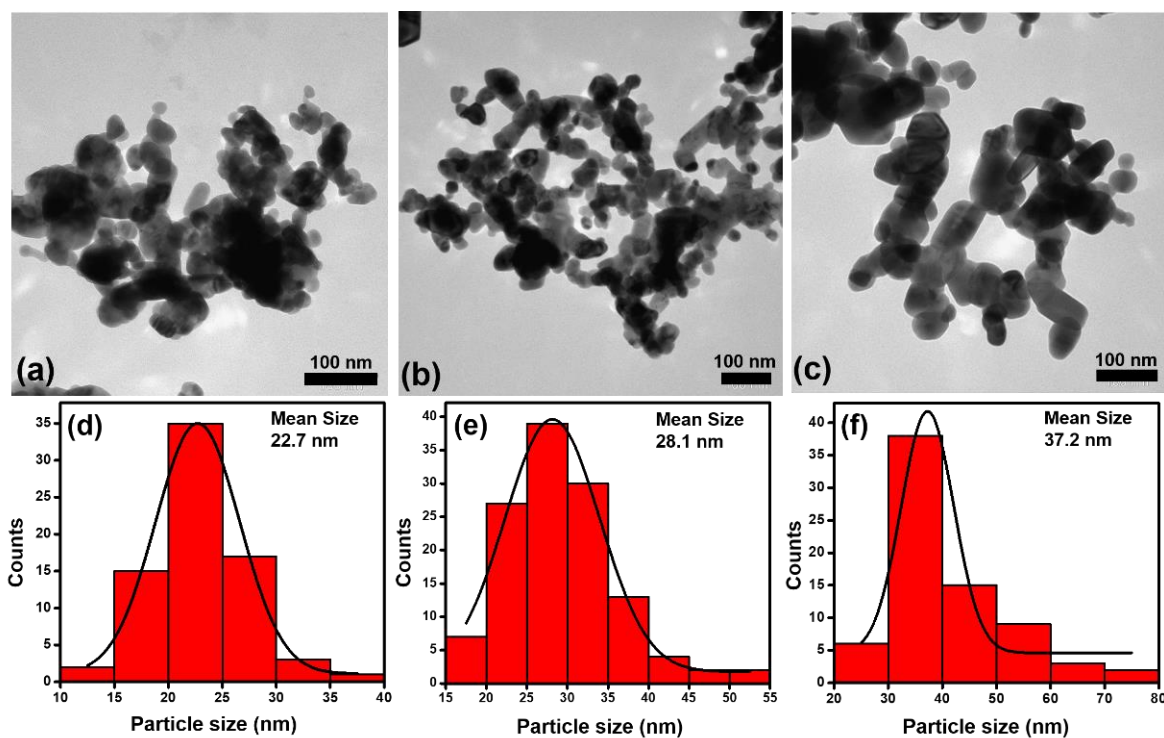


Figure 5. TEM images of $\text{Cu}_x\text{Zn}_y\text{O}$ mixed metal oxide nanoparticles calcined at (a) 350 °C, (b) 450 °C, and (c) 550 °C. Particle size distribution graph obtained from TEM images of (d) 350 °C, (e) 450 °C, and (f) 550 °C.

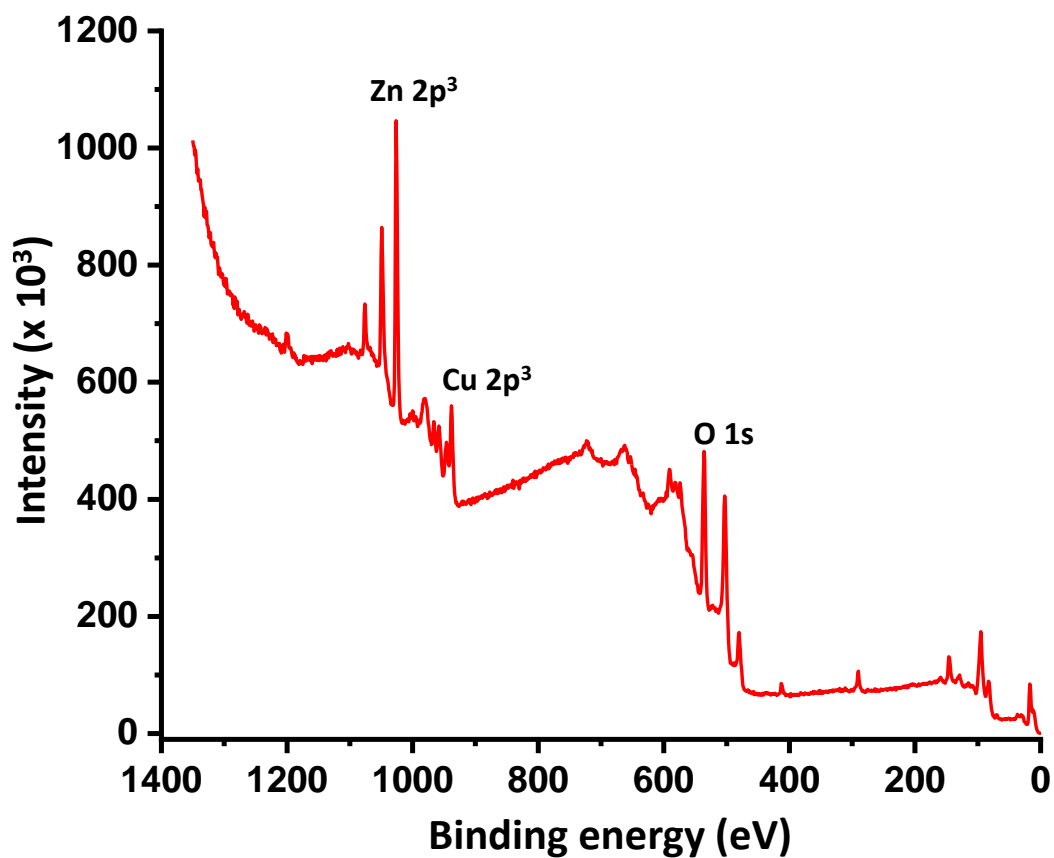


Figure 6. Survey XPS spectrum of $\text{Cu}_x\text{Zn}_y\text{O}$ mixed metal oxide nanoparticles calcined at 450 °C.

3. Discussion

3.1. Catalytic Activity

3.1.1. Effect of Aging Time

The aging time in the preparation of a catalyst affects the catalytic performance of the catalyst [46]; hence, these studies were carried out for the preparation of $\text{Cu}_x\text{Zn}_y\text{O}$ catalysts. In the present study, the catalyst was aged for various time periods, i.e., 2, 4, and 6 h, and then the catalytic performance was tested (Figure 7). Interestingly, it was observed that the catalyst aged at 4 h gave the maximum conversion of toluene to benzaldehyde, i.e., 63.5%. This reaction started with a 10% conversion within the first 10 min of the reaction time. However, the catalysts aged at 2 and 6 h did not show any activity even after 250 min. Therefore, the aging time of 4 h was selected as optimal for the entire study.

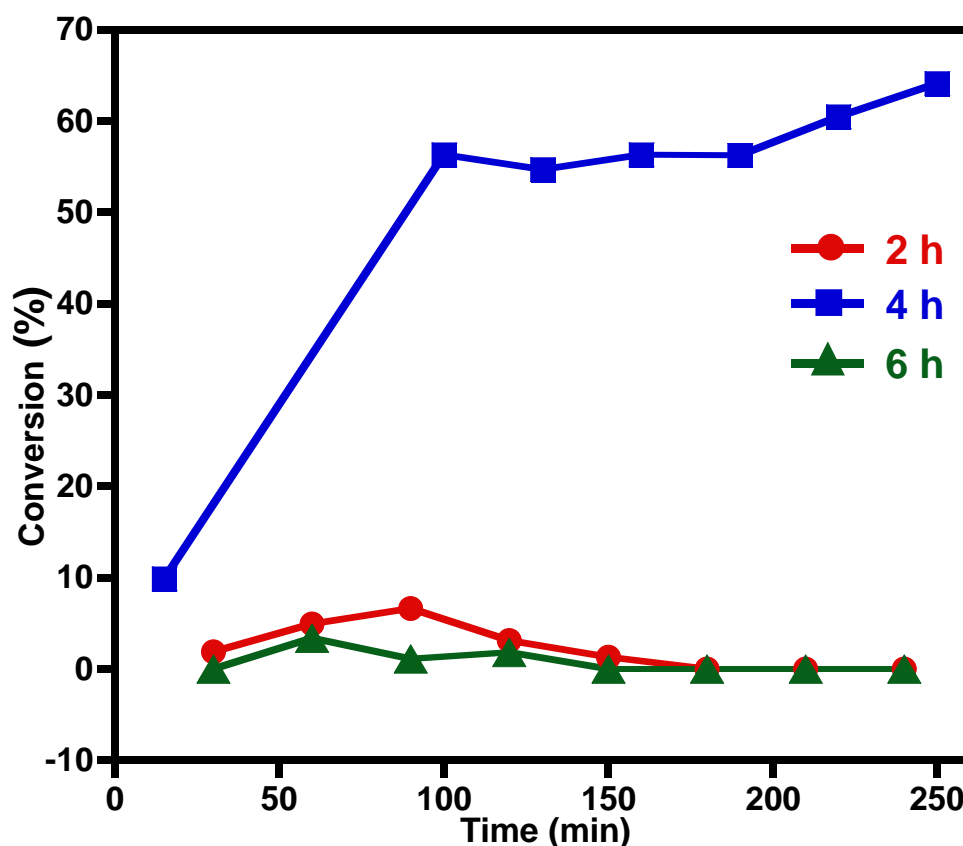


Figure 7. Effect of aging time in the conversion of oxidation of toluene under molecular oxygen using $\text{Cu}_x\text{Zn}_y\text{O}$ mixed metal oxide nanoparticles calcined at 450 °C (conditions: catalyst amount: 0.3 g; toluene flow: 0.01 mL/min; calcination temperature: 450 °C; reaction temperature: 250 °C).

3.1.2. Optimization of Calcination Temperature

The as-synthesized catalyst was calcined at different temperatures, i.e., 350, 450, and 550 °C, for a duration of 24 h and subjected to catalytic evaluation for the conversion of toluene to benzaldehyde. Figure 8 represents the conversion obtained for toluene to benzaldehyde during an oxidation reaction using $\text{Cu}_x\text{Zn}_y\text{O}$ mixed metal oxide nanoparticles calcined at three different temperatures. It can be observed that the catalyst calcined at 350 °C started with a less than 10% conversion product in the first 15 min, and it proceeded to a ~30% conversion within 100 min. Moreover, this catalyst yielded a 54% conversion product, and further continuation of the reaction after this time yielded a product of ~5% conversion. Hence, the reaction was stopped. However, when the catalyst calcined at 450 °C was employed for the same conversion, a 10% conversion product was observed in the first 15 min of the reaction, and then a peak in the conversion performance was

observed in the first 100 min of the reaction, which yielded a 55% conversion product. As the reaction proceeded, catalytic performance was further improved, and finally the 65% conversion product was observed in 250 min of reaction time. Moreover, the catalyst calcined at 550 °C failed to show any conversion throughout the reaction. Hence, it can be considered that the 450 °C calcination temperature was optimum for the best catalytic performance of the prepared catalyst.

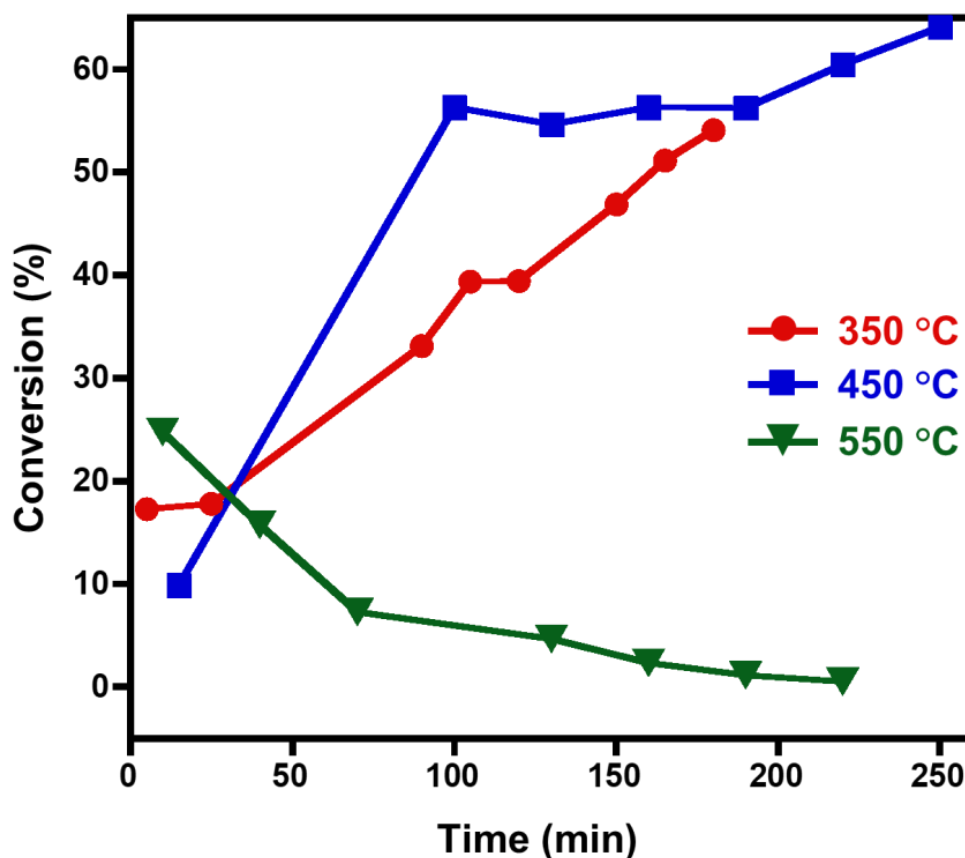


Figure 8. Effect of calcination temperature on the conversion of toluene to benzaldehyde (conditions: catalyst amount: 0.3 g; toluene flow: 0.01 mL/min; reaction temperature: 250 °C).

3.1.3. Optimization of Flow Rate

For this study, the reaction was carried out at two different flow rates of toluene, i.e., 0.01 and 0.02 mL/min (Figure 9). Interestingly, it was found that when the 0.01 mL/min flow rate of toluene was used, the conversion began after 15 min of the reaction. The catalytic performance improved with time, and after 250 min of reaction time, the result was a 65% conversion product.

3.1.4. Extended Catalytic Activity Evaluation

A reactor run for an extended period was carried out in order to ascertain the activity of the catalyst $\text{Cu}_x\text{Zn}_y\text{O}$; the percentage of toluene conversion obtained is illustrated in Figure 10. It can be observed that the reaction yielded a successful conversion. It can be observed that the reaction started with a 39% conversion of toluene to benzaldehyde, which further increased. However, as the reaction proceeded, traces of benzyl alcohol (<5%) were also formed along with benzaldehyde for a short duration, and the selectivity of the catalyst returned to >99%. The catalyst displayed stable efficiency for up to 600 min of reaction time with steady conversion in the range of 55–59% from 210 to 600 min of reaction time. However, after 600 min of reaction time, there was a decline in catalytic activity, yielding a 28% conversion product after 780 min of reaction time. Hence, the

reaction was discontinued after this time. The decline in the catalytic performance of the catalyst, i.e., $\text{Cu}_x\text{Zn}_y\text{O}$, may be due to the coking of the active sites, which shall be studied in the future.

When the results obtained in this study are compared with results previously obtained for the preparation of benzaldehyde by toluene oxidation, it can be noted (Table 2) that various catalysts have given varying conversion products. For example, Okunaka et al. used the catalyst BiVO_4 loaded with Pd (0.1%) under blue-green light, and this method led to an 85% conversion product [47]. In another study, Deng and coworkers employed hexadecylphosphate acid (HDEPA)-terminated mixed oxide nanoparticles for the selective oxidation of toluene to benzaldehyde; an ~83% yield of benzaldehyde was obtained, and the catalyst HDEPA-(Fe_2O_3 -NiO)/ Al_2O_3 possessed a >99% selectivity to benzaldehyde [48]. In another study reported by Shi et al., CoO_x immobilized on SiO_2 was prepared and employed for a similar study. A 91% toluene conversion was observed, but the selectivity to benzaldehyde was found to be as low as 68%. Moreover, this reaction employed N-hydroxyphthalimide and hexafluoropropan-2-ol as promoters, which have to be separated from the product obtained at a later stage [49]. A complex hybrid polyoxometalate photocatalyst, i.e., $\text{K}_6(\text{H}_2\text{O})_8\text{H}_{24}(\text{C}_{26}\text{H}_{16}\text{N}_4\text{O}_4)_8[\text{P}_6\text{W}_{48}\text{Fe}_6\text{O}_{180}] \cdot 6\text{H}_2\text{O}$ (FeW-DPNDI), was employed by Li et al. [50], which led to a 62.5% benzaldehyde yield. V-Mo-Fe-O mixed oxide yielded a maximum of 40.3% toluene conversion with an 84.5% selectivity towards benzaldehyde. However, the catalytic performance depreciated after just 20 min of reaction time [51].

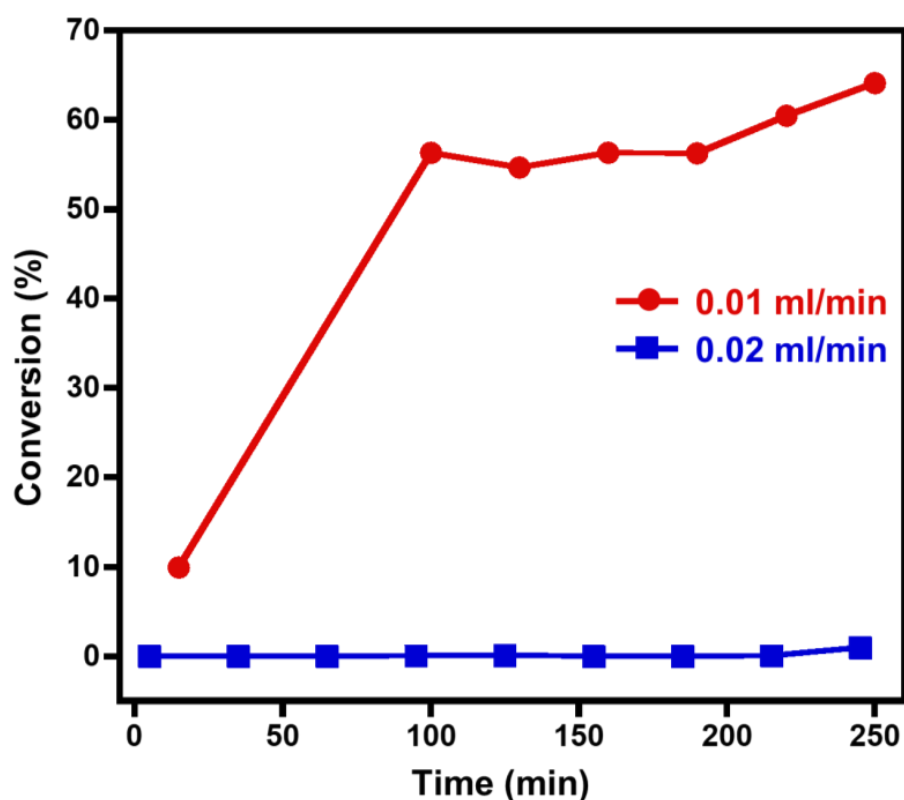


Figure 9. Effect of toluene flow rate on catalytic performance (conditions: catalyst amount: 0.3 g; calcination temperature: 450 °C; reaction temperature: 250 °C).

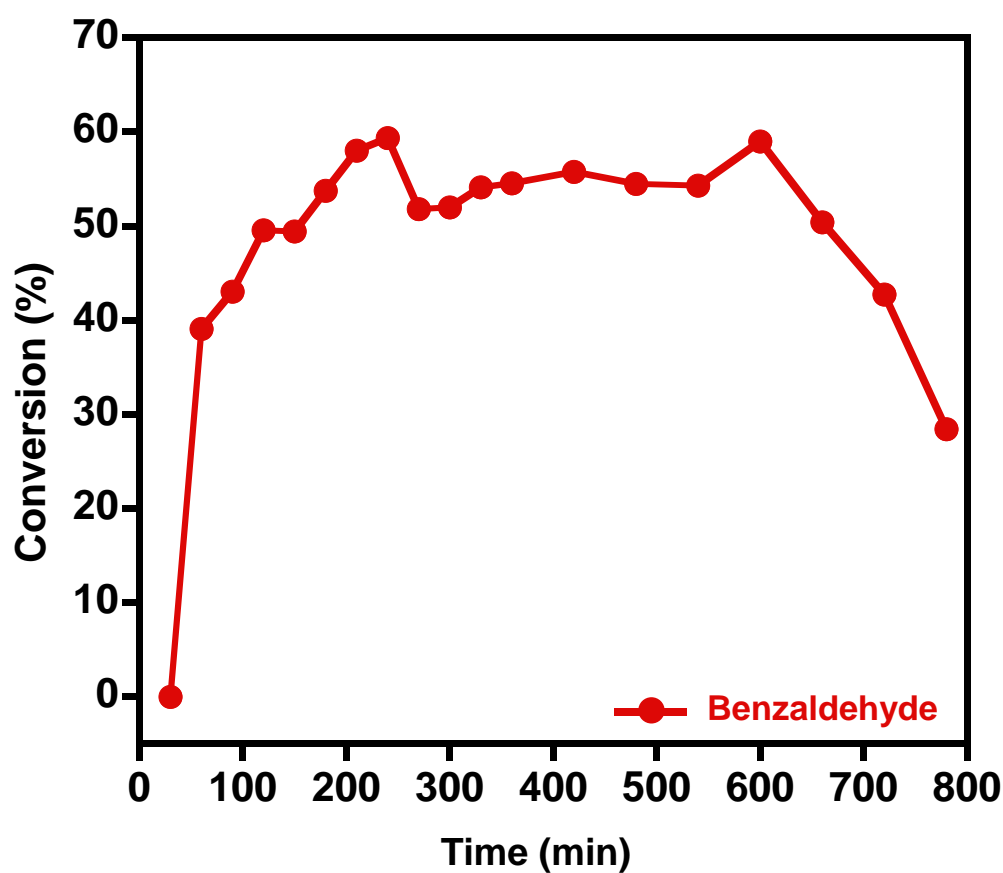


Figure 10. Graphical illustration of the conversion of toluene to benzaldehyde obtained during the catalytic evaluation using $\text{Cu}_x\text{Zn}_y\text{O}$ (conditions: catalyst amount: 0.3 g; toluene flow: 0.01 mL/min; calcination temperature: 450 °C; reaction temperature: 250 °C).

Table 2. Comparison with previously reported catalysts for the oxidation of toluene.

Sl. No.	Catalyst	Temp (°C)	Time	Conversion (%)	Selectivity (%)	Conversion/g/h	Ref.
1	$\text{Cu}_x\text{Zn}_y\text{O}$	250	4 h	60	>99	60/0.3/4	herein
2	$\text{Pd}(0.1\%)/\text{BiVO}_4$	25	15 h	85	>90	85/0.01/15	[47]
3	$\text{HDPa}-(\text{Fe}_2\text{O}_3\text{-NiO})/\text{Al}_2\text{O}_3$	180	4 h	83	>99	83/0.06/4	[48]
4	$\text{CoO}_x/\text{SiO}_2$	25	4 h	91	68	91/0.005/4	[49]
5	$\text{K}_6(\text{H}_2\text{O})_8\text{H}_{24}(\text{C}_{26}\text{H}_{16}\text{N}_4\text{O}_4)_8$ [$\text{P}_6\text{W}_{48}\text{Fe}_6\text{O}_{180}$] $\cdot 6\text{H}_2\text{O}$ (FeW-DPNDI)	25	24 h	62.5	>90	62.5/.016/24	[50]
6	V-Mo-Fe-O	80	0.5 h	40.3	>84	40.3/0.2/0.5	[51]

4. Materials and Methods

4.1. Synthesis of $\text{Cu}_x\text{Zn}_y\text{O}$ Mixed Metal Oxide Nanoparticles

Stoichiometric quantities of 0.1 M copper nitrate (99.95%, Aldrich Chemicals, St. Louis, MI, USA) solution (200 mL, aqueous) and 0.1 M zinc nitrate (99.95%, Aldrich Chemicals, St. Louis, MI, USA) solution (100 mL, aqueous) were mixed in a round-bottom flask attached with a mechanical stirrer, and the temperature of the reaction vessel was gradually increased to 90 °C. Once the temperature was attained, 1 M sodium carbonate (Aldrich Chemicals, St. Louis, MI, USA) solution (aqueous) was added dropwise until the pH became 8. The reaction was later continued for 2, 4, and 6 h at the same temperature. The

solution was kept stirring overnight at room temperature. Finally, the precipitate obtained was washed using deionized (DI) water and dried in an oven at 60 °C overnight. The resulting powder was then calcined in air at different temperatures, namely 350, 450, and 550 °C, with a heating rate of 10 °C/min for 24 h.

4.2. Characterization of Nanoparticles

The crystal structure of the synthesized nanomaterials was confirmed using powder X-ray diffraction techniques on a Bruker D2 Phaser (Bruker, Karlsruhe, Germany) X-ray diffractometer with Cu K α radiation ($\lambda = 1.5418 \text{ \AA}$). Thermogravimetric analysis (TGA) was performed by heating the samples in N₂ flow using a NETZSCH STA 449F3 (Netzsch, Selb, Germany) with a heating rate of 10 °C/min. The structural morphology and the elemental composition of the synthesized nanomaterials were studied using scanning electron microscopy (SEM) and energy-dispersive X-ray analysis (EDX) on a JEOL SEM model JSM 6380 LA (Tokyo, Japan). The shape and size of the nanomaterials were analyzed using a transmission electron microscope (TEM), JEOL TEM model JEM-1011 (Tokyo, Japan). XPS spectra were measured on a PHI 5600 Multi-Technique XPS (Physical Electronics, Lake Drive East, Chanhassen, MN, USA) using monochromatized Al K α at 1486.6 eV.

4.3. Catalytic Activity of Cu_xZn_yO Mixed Metal Oxide Nanoparticles

The oxidation of toluene was carried out in O₂ flow at a temperature of 250 °C under atmospheric pressure in a down-flow stainless steel fixed-bed reactor (length 40 cm and diameter 0.9 cm) with online gas chromatography (GC) analysis (Varian 3800 instrument with a 30 m \times 0.25 mm \times 0.5 μ m HP-INNOWAX capillary column and a flame ionization detector). The temperature in the reactor was controlled by a Eurotherm controller using a thermocouple placed at the top of the catalyst bed. Toluene was injected using an HPLC pump fitted to the fixed-bed reactor. The reactor was packed with 0.3 g of the synthesized material (powder) through which the toluene (98%, 0.01–0.02 mL/min) and oxygen (20 mL/min) were allowed to flow. The downstream products were analyzed through the GC connected online to continuously monitor the conversion of toluene.

5. Conclusions

Based on the findings of this research work and in comparison to the previously reported catalysts for the same conversion, it can be concluded that the catalyst presented herein, i.e., Cu_xZn_yO, prepared by a simple co-precipitation method, is a suitable catalyst for the facile conversion of toluene to benzaldehyde. The catalyst was found to be composed of mixed phases of hexagonal and monoclinic crystal structures. The catalyst calcined at different temperatures yielded nanoparticles of varying sizes. The catalyst calcined at 550 °C was found to possess a particle size of ~40 nm, whereas the catalysts calcined at 350 and 450 °C showed sizes of around 23 and 30 nm, respectively. The catalysts obtained were found to be effective for the conversion of toluene to benzaldehyde with a ~65% conversion product and >99% selectivity towards benzaldehyde. It appears that the most effective catalysts are in this range, and a slightly higher particle size of around 40 nm makes the material less effective. It can be concluded that the size of nanoparticles plays the most significant role in the selective oxidation of toluene to benzaldehyde. The catalyst was also found to be effective for ~14 h. Further studies towards improving the conversion while maintaining the selectivity are being planned and shall be reported later.

Author Contributions: A.A. and M.R.H.S. designed the project; A.A. and K.H.A. helped to write the manuscript; A.B.A.A. performed the experiments and some parts of the characterization; K.H.A., project administration; K.H.A., funding acquisition; A.A. and M.R.H.S. provided scientific guidance for successful completion of the project and helped to draft the manuscript. All authors have read and agreed to the published version of the manuscript.

Funding: This work was supported by the Deanship of Scientific Research (DRS), King Abdulaziz University, Jeddah, under grant no. (G: 1482-665-1440). The authors, therefore, gratefully acknowledge the technical and financial support provided by the DRS.

Data Availability Statement: Not applicable.

Conflicts of Interest: The authors declare there is no conflict of interest.

References

1. Partenheimer, W. Methodology and scope of metal/bromide autoxidation of hydrocarbons. *Catal. Today* **1995**, *23*, 69–158. [[CrossRef](#)]
2. Romero, A.; Irigoyen, B.; Larrondo, S.; Jacobo, S.; Amadeo, N. Effect of Fe doped over V–Sb oxide catalyst in toluene selective oxidation. *Catal. Today* **2008**, *133–135*, 775–779. [[CrossRef](#)]
3. Deori, K.; Kalita, C.; Deka, S. (100) surface-exposed CeO₂ nanocubes as an efficient heterogeneous catalyst in the tandem oxidation of benzyl alcohol, para-chlorobenzyl alcohol and toluene to the corresponding aldehydes selectively. *J. Mater. Chem. A* **2015**, *3*, 6909–6920. [[CrossRef](#)]
4. Mal, D.D.; Khilari, S.; Pradhan, D. Efficient and selective oxidation of toluene to benzaldehyde on manganese tungstate nanobars: A noble metal-free approach. *Green Chem.* **2018**, *20*, 2279–2289. [[CrossRef](#)]
5. Mao, Y.; Bakac, A. Photocatalytic Oxidation of Toluene to Benzaldehyde by Molecular Oxygen. *J. Phys. Chem.* **1996**, *100*, 4219–4223. [[CrossRef](#)]
6. Satrio, J.A.; Doraiswamy, L. Production of benzaldehyde: A case study in a possible industrial application of phase-transfer catalysis. *Chem. Eng. J.* **2001**, *82*, 43–56. [[CrossRef](#)]
7. Li, L.; Zhao, J.; Yang, J.; Fu, T.; Xue, N.; Peng, L.; Guo, X.; Ding, W. A sintering-resistant Pd/SiO₂ catalyst by reverse-loading nano iron oxide for aerobic oxidation of benzyl alcohol. *RSC Adv.* **2015**, *5*, 4766–4769. [[CrossRef](#)]
8. Savara, A.; Chan-Thaw, C.E.; Rossetti, I.; Villa, A.; Prati, L. Benzyl Alcohol Oxidation on Carbon-Supported Pd Nanoparticles: Elucidating the Reaction Mechanism. *ChemCatChem* **2014**, *6*, 3464–3473. [[CrossRef](#)]
9. Veisi, H.; Nikseresht, A.; Mohammadi, S.; Hemmati, S. Facile in-situ synthesis and deposition of monodisperse palladium nanoparticles on polydopa-mine-functionalized silica gel as a heterogeneous and recyclable nanocatalyst for aerobic oxidation of alcohols. *Chin. J. Catal.* **2018**, *39*, 1044–1050. [[CrossRef](#)]
10. Li, W.; Ye, H.; Liu, G.; Ji, H.; Zhou, Y.; Han, K. The role of graphene coating on cordierite-supported Pd monolithic catalysts for low-temperature combustion of toluene. *Chin. J. Catal.* **2018**, *39*, 946–954. [[CrossRef](#)]
11. Assal, M.E.; Kuniyil, M.; Khan, M.; Al-Warthan, A.; Siddiqui, M.R.H.; Tremel, W.; Tahir, M.N.; Adil, S.F. Synthesis and Comparative Catalytic Study of Zirconia-MnCO₃ or -Mn₂O₃ for the Oxidation of Benzylic Alcohols. *ChemistryOpen* **2017**, *6*, 112–120. [[CrossRef](#)] [[PubMed](#)]
12. Assal, M.E.; Shaik, M.R.; Kuniyil, M.; Khan, M.; Al-Warthan, A.; Siddiqui, M.R.H.; Khan, S.M.A.; Tremel, W.; Nawaz Tahir, M.; Adil, S.F. A highly reduced graphene oxide/ZrOx–MnCO₃ or–Mn₂O₃ nanocomposite as an efficient catalyst for selective aerial oxidation of benzylic alcohols. *RSC Adv.* **2017**, *7*, 55336–55349. [[CrossRef](#)]
13. Adil, S.F.; Assal, M.E.; Shaik, M.R.; Kuniyil, M.; Al Otaibi, N.M.; Khan, M.; Sharif, M.; Alam, M.M.; Al-Warthan, A.; Ali Mohammed, J.; et al. A Facile Synthesis of ZrOx–MnCO₃/Graphene Oxide (GRO) Nanocomposites for the Oxidation of Alcohols using Molecular Oxygen under Base Free Conditions. *Catalysts* **2019**, *9*, 759. [[CrossRef](#)]
14. Kuniyil, M.; Kumar, J.V.S.; Adil, S.F.; Assal, M.E.; Shaik, M.R.; Khan, M.; Al-Warthan, A.; Siddiqui, M.R.H.; Khan, A.; Bilal, M.; et al. Eco-Friendly and Solvent-Less Mechanochemical Synthesis of ZrO₂–MnCO₃/N-Doped Graphene Nanocomposites: A Highly Efficacious Catalyst for Base-Free Aerobic Oxidation of Various Types of Alcohols. *Catalysts* **2020**, *10*, 1136. [[CrossRef](#)]
15. Wagner, C. The Mechanism of the Decomposition of Nitrous Oxide on Zinc Oxide as Catalyst. *J. Chem. Phys.* **1950**, *18*, 69. [[CrossRef](#)]
16. Menezes, P.W.; Indra, A.; Bergmann, A.; Chernev, P.; Walter, C.; Dau, H.; Strasser, P.; Driess, M. Uncovering the prominent role of metal ions in octahedral versus tetrahedral sites of cobalt–zinc oxide catalysts for efficient oxidation of water. *J. Mater. Chem. A* **2016**, *4*, 10014–10022. [[CrossRef](#)]
17. Singh, B.; Long, J.R.; Fabrizi de Biani, F.; Gatteschi, D.; Stavropoulos, P. Synthesis, reactivity, and catalytic behavior of iron/zinc-containing species involved in oxidation of hydro-carbons under Gif-type conditions. *J. Am. Chem. Soc.* **1997**, *119*, 7030–7047. [[CrossRef](#)]
18. Priyanka; Srivastava, V.C. Photocatalytic Oxidation of Dye Bearing Wastewater by Iron Doped Zinc Oxide. *Ind. Eng. Chem. Res.* **2013**, *52*, 17790–17799. [[CrossRef](#)]
19. Adil, S.F.; Assal, M.E.; Kuniyil, M.; Khan, M.; Shaik, M.R.; Al-Warthan, A.; Labis, J.P.; Siddiqui, M.R.H. Synthesis and Comparative Catalytic Study of Zinc Oxide (ZnOx) Nanoparticles Promoted MnCO₃, MnO₂ and Mn₂O₃ for Selective Oxidation of Benzylic Alcohols Using Molecular Oxygen. *Mater. Express* **2017**, *7*, 79–92. [[CrossRef](#)]
20. Assal, M.E.; Shaik, M.R.; Kuniyil, M.; Khan, M.; Alzahrani, A.Y.; Al-Warthan, A.; Siddiqui, M.R.H.; Adil, S.F. Mixed Zinc/Manganese on Highly Reduced Graphene Oxide: A Highly Active Nanocomposite Catalyst for Aerial Oxidation of Benzylic Alcohols. *Catalysts* **2017**, *7*, 391. [[CrossRef](#)]

21. Adil, S.F.; Assal, M.E.; Shaik, M.R.; Kuniyil, M.; Hashmi, A.; Khan, M.; Khan, A.; Tahir, M.N.; Al-Warthan, A.; Siddiqui, M.R.H. Efficient aerial oxidation of different types of alcohols using ZnO nanoparticle–MnCO₃–graphene oxide composites. *Appl. Organomet. Chem.* **2020**, *34*. [[CrossRef](#)]
22. Kuniyil, M.; Shanmukha Kumar, J.V.; Adil, S.F.; Assal, M.E.; Shaik, M.R.; Khan, M.; Al-Warthan, A.; Siddiqui, M.R.H. Production of biodiesel from waste cooking oil using ZnCuO/N-doped graphene nanocomposite as an efficient heterogeneous catalyst. *Arab. J. Chem.* **2021**, *14*, 102982. [[CrossRef](#)]
23. Li, Y.; Gan, L.; Si, R. Effect of tungsten oxide on ceria nanorods to support copper species as CO oxidation catalysts. *J. Rare Earths* **2021**, *39*, 43–50. [[CrossRef](#)]
24. Lee, H.J.; Yang, J.H.; You, J.H.; Yoon, B.Y. Sea-urchin-like mesoporous copper-manganese oxide catalysts: Influence of copper on benzene oxidation. *J. Ind. Eng. Chem.* **2020**, *89*, 156–165. [[CrossRef](#)]
25. Mishra, S.; Bal, R.; Dey, R. Heterogeneous recyclable copper oxide supported on activated red mud as an efficient and stable catalyst for the one pot hydroxylation of benzene to phenol. *Mol. Catal.* **2021**, *499*, 111310. [[CrossRef](#)]
26. Adil, S.F.; Alabbad, S.; Kuniyil, M.; Khan, M.; Alwarthan, A.; Mohri, N.; Tremel, W.; Nawaz Tahir, M.; Rafiq, M.; Siddiqui, H. Vanadia Supported on Nickel Manganese Oxide Nanocatalysts for the Catalytic Oxidation of Aromatic Alcohols. *Nanoscale Res. Lett.* **2015**, *10*, 1–9. [[CrossRef](#)]
27. Sultana, S.; Kishore, D.; Kuniyil, M.; Khan, M.; Alwarthan, A.; Prasad, K.; Labis, J.P.; Adil, S.F. Ceria doped mixed metal oxide nanoparticles as oxidation catalysts: Synthesis and their characterization. *Arab. J. Chem.* **2015**, *8*, 766–770. [[CrossRef](#)]
28. Khan, M.; Khan, M.; Kuniyil, M.; Adil, S.F.; Al-Warthan, A.; Alkhatlan, H.Z.; Tremel, W.; Nawaz Tahir, M.; Siddiqui, M.R.H. Biogenic synthesis of palladium nanoparticles using *Pulicaria glutinosa* extract and their catalytic activity towards the Suzuki coupling reaction. *Dalton Trans.* **2014**, *43*, 9026–9031. [[CrossRef](#)]
29. Khan, M.; Albalawia, G.H.; Shaik, M.R.; Khan, M.; Adil, S.F.; Kuniyil, M.; Alkhatlan, H.Z.; Al-Warthan, A.; Siddiqui, M.R.H. Miswak mediated green synthesized palladium nanoparticles as effective catalysts for the Suzuki coupling reactions in aqueous media. *J. Saudi Chem. Soc.* **2017**, *21*, 450–457. [[CrossRef](#)]
30. Bowker, M.; Hadden, R.A.; Houghton, H.; Hyland, J.N.K.; Waugh, K.C. ChemInform Abstract: The Mechanism of Methanol Synthesis on Copper/Zinc Oxide/Alumina Catalysts. *ChemInform* **1988**, *19*, 263–273. [[CrossRef](#)]
31. Taylor, S.H.; Hutchings, G.J.; Mirzaei, A.A. Copper zinc oxide catalysts for ambient temperature carbon monoxide oxidation. *Chem. Commun.* **1999**, *1999*, 1373–1374. [[CrossRef](#)]
32. Whittle, D.M.; Mirzaei, A.A.; Hargreaves, J.S.J.; Joyner, R.W.; Kiely, C.J.; Taylor, S.H.; Hutchings, G.J. Co-precipitated copper zinc oxide catalysts for ambient temperature carbon monoxide oxidation: Effect of precipitate ageing on catalyst activity. *Phys. Chem. Chem. Phys.* **2002**, *4*, 5915–5920. [[CrossRef](#)]
33. Huang, T.-J.; Chren, S.-L. Kinetics of partial oxidation of methanol over a copper-zinc catalyst. *Appl. Catal.* **1988**, *40*, 43–52. [[CrossRef](#)]
34. Chaudhuri, P.; Hess, M.; Müller, J.; Hildenbrand, K.; Bill, E.; Weyhermüller, T.; Wieghardt, K. Aerobic Oxidation of Primary Alcohols (Including Methanol) by Copper (II)– and Zinc (II)–Phenoxy Radical Catalysts. *J. Am. Chem. Soc.* **1999**, *121*, 9599–9610. [[CrossRef](#)]
35. Sharma, R.K.; Ghose, R. Synthesis of nanocrystalline CuO–ZnO mixed metal oxide powder by a homogeneous precipitation method. *Ceram. Int.* **2014**, *40*, 10919–10926. [[CrossRef](#)]
36. Al-Zaqri, N.; Alsalmeh, A.; Adil, S.F.; Alsaleh, A.; Alshammari, S.G.; Alresayes, S.I.; Alotaibi, R.; Al-Kinany, M.; Siddiqui, M.R.H. Comparative catalytic evaluation of nickel and cobalt substituted phosphomolybdic acid catalyst supported on silica for hydrodesulfurization of thiophene. *J. Saudi Chem. Soc.* **2017**, *21*, 965–973. [[CrossRef](#)]
37. Boddapati, S.N.M.; Tamminana, R.; Gollapudi, R.K.; Nurbasha, S.; Assal, M.E.; Alduhaish, O.; Siddiqui, M.R.H.; Bollikolla, H.B.; Adil, S.F. Copper-Promoted One-Pot Approach: Synthesis of Benzimidazoles. *Molecules* **2020**, *25*, 1788. [[CrossRef](#)]
38. Khan, M.; Kuniyil, M.; Shaik, M.R.; Khan, M.; Adil, S.F.; Al-Warthan, A.; Alkhatlan, H.Z.; Tremel, W.; Tahir, M.N.; Siddiqui, M.R.H. Plant Extract Mediated Eco-Friendly Synthesis of Pd@Graphene Nanocatalyst: An Efficient and Reusable Catalyst for the Suzuki-Miyaura Coupling. *Catalysts* **2017**, *7*, 20. [[CrossRef](#)]
39. Ahmad, N.; Alam, M.; Adil, S.F.; Ansari, A.A.; Assal, M.E.; Ramay, S.M.; Ahmed, M.; Alam, M.M.; Siddiqui, M.R.H. Synthesis, characterization, and selective benzyl alcohol aerobic oxidation over Ni-loaded BaFeO₃ meso-porous catalyst. *J. King Saud Univ. Sci.* **2020**, *32*, 2059–2068. [[CrossRef](#)]
40. Assal, M.E.; Kuniyil, M.; Shaik, M.R.; Khan, M.; Al-Warthan, A.; Siddiqui, M.R.H.; Adil, S.F. Synthesis, Characterization, and Relative Study on the Catalytic Activity of Zinc Oxide Nanoparticles Doped MnCO₃–MnO₂, and–Mn₂O₃ Nanocomposites for Aerial Oxidation of Alcohols. *J. Chem.* **2017**, *2017*. [[CrossRef](#)]
41. Khan, M.; Shaik, M.R.; Adil, S.F.; Kuniyil, M.; Ashraf, M.; Frerichs, H.; Sarif, M.A.; Siddiqui, M.R.H.; Al-Warthan, A.; Labis, J.P.; et al. Facile synthesis of Pd@graphene nanocomposites with enhanced catalytic activity towards Suzuki coupling reaction. *Sci. Rep.* **2020**, *10*, 1–14. [[CrossRef](#)]
42. Alduhaish, O.; Adil, S.F.; Assal, M.E.; Shaik, M.R.; Kuniyil, M.; Manqari, K.M.; Sekou, D.; Khan, M.; Khan, A.; Dewidar, A.Z. Synthesis and Characterization of CoxOy–MnCO₃ and CoxOy–Mn₂O₃ Catalysts: A Comparative Catalytic Assessment Towards the Aerial Oxidation of Various Kinds of Alcohols. *Processes* **2020**, *8*, 910. [[CrossRef](#)]
43. Shuai, M.; Liao, L.; Lu, H.B.; Zhang, L.; Li, J.C.; Fu, D.J. Room-temperature ferromagnetism in Cu⁺ implanted ZnO nanowires. *J. Phys. D Appl. Phys.* **2008**, *41*, 135010. [[CrossRef](#)]

44. Li, Z.; Chen, H.; Liu, W. Full-Spectrum Photocatalytic Activity of ZnO/CuO/ZnFe₂O₄ Nanocomposite as a PhotoFenton-Like Catalyst. *Catalysts* **2018**, *8*, 557. [[CrossRef](#)]
45. Xu, D.; Fan, D.; Shen, W. Catalyst-free direct vapor-phase growth of Zn_{1-x}Cu_xO micro-cross structures and their optical properties. *Nanoscale Res. Lett.* **2013**, *8*, 46. [[CrossRef](#)]
46. Jeong, Y.; Kim, I.; Kang, J.Y.; Yan, N.; Jeong, H.; Park, J.K.; Park, J.H.; Jung, J.C. Effect of the aging time of the precipitate on the activity of Cu/ZnO catalysts for alcohol-assisted low temperature methanol synthesis. *J. Mol. Catal. A Chem.* **2016**, *418*, 168–174. [[CrossRef](#)]
47. Okunaka, S.; Tokudome, H.; Hitomi, Y. Selective oxidation of toluene to benzaldehyde over Pd/BiVO₄ particles under blue to green light irradiation. *J. Catal.* **2020**, *391*, 480–484. [[CrossRef](#)]
48. Deng, C.; Xu, M.; Dong, Z.; Li, L.; Yang, J.; Guo, X.; Peng, L.; Xue, N.; Zhu, Y.; Ding, W. Exclusively catalytic oxidation of toluene to benzaldehyde in an O/W emulsion stabilized by hexa-decylphosphate acid terminated mixed-oxide nanoparticles. *Chin. J. Catal.* **2020**, *41*, 341–349. [[CrossRef](#)]
49. Shi, G.; Xu, S.; Bao, Y.; Xu, J.; Liang, Y. Selective aerobic oxidation of toluene to benzaldehyde on immobilized CoO_x on SiO₂ catalyst in the presence of N-hydroxyphthalimide and hexafluoropropan-2-ol. *Catal. Commun.* **2019**, *123*, 73–78. [[CrossRef](#)]
50. Li, J.; He, J.; Si, C.; Li, M.; Han, Q.; Wang, Z.; Zhao, J. Special-selective C–H oxidation of toluene to benzaldehyde by a hybrid polyoxometalate photocatalyst including a rare [P6W48Fe₆O₁₈₀]³⁰⁻ anion. *J. Catal.* **2020**, *392*, 244–253. [[CrossRef](#)]
51. Xia, H.; Liu, Z.; Xu, Y.; Zuo, J.; Qin, Z. Highly efficient V-Mo-Fe-O catalysts for selective oxidation of toluene to benzaldehyde. *Catal. Commun.* **2016**, *86*, 72–76. [[CrossRef](#)]